A general framework for pellet reactor modelling : application to P-recovery

Ludovic Montastruc, Catherine Azzaro-Pantel, Béatrice Biscans, Michel Cabassud, Serge Domenech, Luc Pibouleau

A GENERAL FRAMEWORK FOR PELLET REACTOR MODELLING: APPLICATION TO P-RECOVERY

L. MONTASTRUC, C. AZZARO-PANTEL, B. BISCANS, M. CABASSUD, S. DOMENECH and L. DIBOULEAU

Laboratoire de Génie Chimique, UMR 5503, Toulouse, France

Emphasis in recent years has been focused on improving processes which lead to enhanced phosphate recovery. This paper studies the precipitation features of calcium phosphate in a fluidized bed reactor in a concentration range between 4 and 50 mg l^{-1} and establishes the conditions for optimum phosphate removal efficiency. For this purpose, two models are coupled for predicting the pellet reactor efficiency. First, a thermodynamical model is used for predicting calcium phosphate precipitation vs. initial conditions (pH, [P], [Ca], temperature). The second one is a reactor network model. Its parameters are identified by an optimization procedure based on simulated annealing and quadratic programming. The efficiency is computed by coupling a simple agglomeration model with a combination of elementary systems representing basic ideal flow patterns (perfect mixed flow, plug flow, etc.). More precisely, the superstructure represents the hydrodynamical conditions in the fluidized bed. The observed results show that a simple combination of ideal flow patterns is involved in pellet reactor modelling, which seems interesting for a future control. The experimental prototype used for validation purpose is first described. Then, the thermochemical model is presented for calcium phosphate precipitation. The third part is devoted to the reactor network-oriented model. The approach presented is finally validated with experimental runs.

Keywords: pellet reactor; calcium phosphate precipitation; wastewater.

INTRODUCTION

The need to limit phosphate emission in the environment has diverted attention in recent years to processes which lead to the recovery of phosphate. Phosphorus can be found under various chemical forms in urban wastewater, which represents about 30–50% of the total waste of P: insoluble or dissolved organic phosphorus, orthophosphates (up to 70% sometimes) and condensed inorganic phosphates. In France, the average concentration of phosphorus in domestic wastewater is within the range 15–25 mg l^{-1}, which may vary from day to day, even during the day. The P-discharge in the aqueous natural environment leads to excessive development of algae and to a pH increase, thus contributing to eutrophication. Consequently, phosphorus reduction in rivers is considered as a key factor in the fight against pollution. The principal legislative tool in Europe for fighting eutrophication is the EC Urban Waste Water Treatment Directive (271/91/EEC). This action came into force in 1991 and enabled waterbodies to be classified as Sensitive Areas if they displayed symptoms of eutrophication. The precipitation of phosphate salts is a means of P recovery in effluents with a low concentration of inorganic phosphorus. In recent years, several works have studied calcium phosphate precipitation in the so-called pellet reactor (Seckler *et al.*, 1996; Hirasawa and Toya, 1990).

The purpose of the study presented in this paper is to develop a methodology based on modelling for optimization of the pellet reactor efficiency. The experimental prototype used for validation purposes is first described. Then, the thermochemical model is presented for calcium phosphate precipitation. The third part is devoted to the reactor network-oriented model. The approach presented is finally validated with experimental runs.

PROCESS DESCRIPTION

The process is based on calcium phosphate precipitation obtained by mixing a phosphate solution with calcium ions and a base. More precisely, it involves a fluidized bed of sand continuously fed with aqueous solutions (see Figure 1). Calcium phosphate precipitates on the surface of sand grains. At the same time, small particles, 'fines', leave the bed with the remaining phosphate not recovered in the reactor. A layer of fines which has agglomerated is observed at the upper zone of the fluidized bed. Both total and dissolved concentrations of phosphorus, pH and temperature were measured at the outlet stream. The temperature was kept constant during the experimental runs. In order to measure the dissolved P concentrations, the upper outlet stream was filtered immediately over a 0.45 μm filter and analysed. Another sample was pre-treated with HCl in order

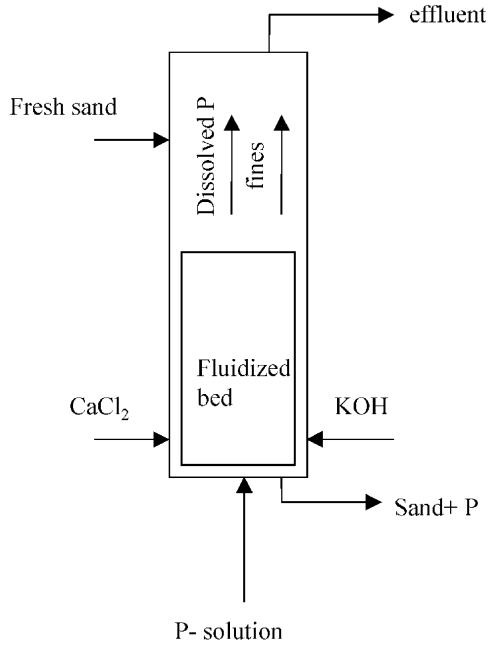

Figure 1. Schematic representation of the pellet reactor.

to dissolve any suspended solid and the total phosphorus amount was measured. The phosphate removal efficiency (η) of the reactor and the conversion of phosphate from the liquid to the solid phase (X) are defined respectively as:

$$\eta = \frac{w_{p,in} - w_{p,tot}}{w_{p,in}} \quad (1)$$

$$X = \frac{w_{p,in} - w_{p,sol}}{w_{p,in}} \quad (2)$$

where $w_{p,in}$ represents the flowrate of the phosphorus component at reactor inlet, $w_{p,tot}$ gives the total flowrate of phosphorus both as dissolved and as fines at reactor outlet and $w_{p,sol}$ is the flowrate of dissolved P at the reactor top outlet. If η_{agg} is the agglomeration rate, that is, the ratio between fines in the bed and in the outlet stream, the following relation can be deduced:

$$\eta = \eta_{agg} X \quad (3)$$

The phosphate-covered grains are removed from the bottom of the bed and replaced intermittently by fresh sand grains. In most studies reported in the literature (Morse *et al.*, 1998), the phosphate removal efficiency of a single pass reactor, even at industrial scale, has an order of magnitude of only 50%. Recall that the pellet reactor efficiency depends not only on pH but also on the hydrodynamic conditions (Montastruc *et al.*, 2002a). Moreover, the conversion rate depends on calcium and phosphate ion concentrations, as well as on supersaturation, ionic strength, temperature, ion types, pH but also on time (solid–solid transformation), as noted in the literature (Baronne and Nancollas, 1977; Van Kemenade and de Bruyn, 1987; Boskey and Posner, 1973).

MODELLING PRINCIPLES

Two models are successively used to compute the reactor efficiency. At the first level (see Figure 2), a thermochemical model determines the quantity of phosphate both in the liquid and solid phases vs. pH value, temperature and calcium concentration. A second modelling step could involve an agglomeration model which requires, as classical parameters (Mullin, 2001), the density value of the precipitated calcium phosphates and fine diameter. Moreover, the agglomeration rate depends on the hydrodynamical conditions, particularly the eddy sizes. These values are difficult to obtain and require a lot of assumptions which are difficult to verify practically. Consequently, another alternative is proposed in this paper to tackle the problem. The two-stage methodology is detailed in what follows.

Thermodynamical Model

Assumptions

Calcium phosphate precipitation is a very complex subject involving various parameters. The different forms of crystallized calcium phosphate are presented in Table 1.

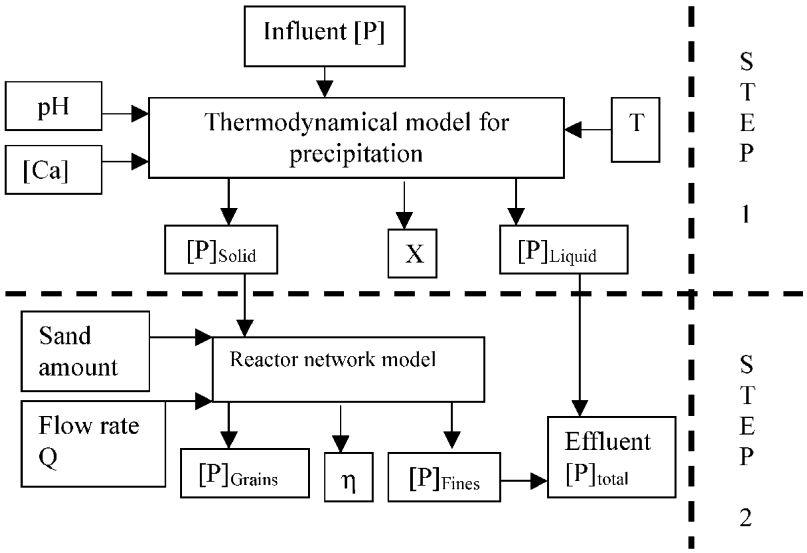

Figure 2. Principles of pellet reactor modelling.

Table 1. Different forms of calcium phosphate.

Name	Formula	p*K*s
Dicalcium phosphate dihydrate (DCPD)	$CaHPO_4{\cdot}2H_2O$	6.69 at 25°C (Freche, 1989) 6.6 at 25°C (Stumm and Morgan, 1981)
Dicalcium phosphate anhydrate (DCPA)	$CaHPO_4$	6.90 at 25°C (Freche, 1989)
Octocalcium phosphate (OCP)	$Ca_4H(PO_4)_3{\cdot}2.5H_2O$	49.60 at 25°C (Freche, 1989)
Tricalcium phosphate (TCP)	$Ca_3(PO_4)_2$	26.00 at 25°C (Ringbom, 1967)
Amorphous calcium phosphate (ACP)	$Ca_3(PO_4)_2$	26.52 at 25°C (Seckler *et al.*, 1996) 25.20 at 20°C (Meyer and Eanes, 1978)
Hydroxyapatite (HAP)	$Ca_{10}(PO_4)_6(OH)_2$	58.33 at 25°C (Freche, 1989)

It is mentioned in the literature (Van Kemenade and de Bruyn, 1987) that phosphate precipitation by calcium salts leads to the formation of both dicalcium phosphate dihydrate (DCPD) and amorphous calcium phosphate (ACP) for a pH value of 7 and only to amorphous calcium phosphate (ACP) within a pH range of 9–10.5. Some experiments carried out in a previous work at a temperature of 26°C (Van Kemenade and de Bruyn, 1987) for a pH range of 6–7.4 followed by the evolution of the different calcium phosphate forms. The observed sequences as a function of pH are described in Table 2.

In each case, Ostwald's rule, which foresees that the least thermodynamically stable phase formed is the first one, is respected. The evolution is not straightforward and a study about the transformation of ACP to HAP (hydroxyapatite; Boskey and Posner, 1973) for a pH range of 6.8–10.0 showed that the required time for total conversion may vary from 1 h for a pH equal to 6.8 to more than 11 h for a pH value equal to 10 (Table 3).

These studies showed that the nature of calcium phosphate precipitate depends on the supersaturation of the various species. However, it can be noted, on the one hand, that the DCPD phase was far less observed due to its relatively weak p*K*s and, on the other hand, that after the initial formation of an amorphous phase, a crystalline HAP phase was observed. Only a single precipitated species, i.e. ACP, was observed (Seckler *et al.*, 1996) for experiments carried out at a pH value higher than 7, a phosphate concentration of $1.6 \times 10^{-3}\,\mathrm{mol\,l^{-1}}$ and a Ca/P molar ratio equal to 3. However, the DCPD and ACP forms were observed in additional experiments using the following conditions, i.e. a pH range within 6–7, an initial phosphate concentration of $3.2 \times 10^{-3}\,\mathrm{mol\,l^{-1}}$ and a Ca/P molar ratio varying from 1 to 7 (Seckler *et al.*, 1996).

Therefore, the hypothesis of the precipitation of both ACP and DCPD seems important to examine within the framework of this work. Since the precipitation was assumed to take place in a pellet reactor, the transformation from ACP to HAP is not possible due to a low residence time (see Table 3).

The phenomena observed during precipitation in a pellet reactor are not the same as in a stirred vessel. In a pellet reactor, the fines produced by nucleation are not maintained in the mother solution for a long time, since the fines are agglomerated in the sand and the liquid (mother solution) flows across the bed. On the other hand, in a stirred vessel after a long time, the produced calcium phosphate is the most stable, i.e. HAP.

Table 2. Transformation of the calcium phosphate crystalline forms.

pH	Transformation
6.0	OCP ⇒ DCPD(⇒) HAP
6.7	DCPD = OCP ⇒ HAP
7.4	ACP ⇒ OCP ⇒ HAP

Equations of the model

The objective is to propose a mathematical model for the computation of the conversion for the system $Ca–PO_4–H_2O$.

To model the evolution of phosphate conversion rate as a function of pH with respect to the different calcium phosphate species precipitation, the mass and electroneutrality conservation balances as well as the supersaturation were taken into account. During this precipitation, the aqueous species considered are, on the one hand, for the phosphoric acid H_3PO_4, $H_2PO_4^-$, HPO_4^{2-}, PO_4^{3-}, and on the other hand the Ca^{2+} ion and the corresponding calcium salts. The $KHPO_4^-$ species is not taken into account in the electroneutrality balance due to the small quantity involved resulting the low values of the dissociation constants.

An investigation was first carried out to identify the species which may contribute to precipitation. This study takes into account HAP, OCP, DCPD and ACP. Figure 3 shows that ACP precipitation represents the experimental points for high pH values (pH > 7.3) and this result agrees with ACP presence during precipitation. But, for pH values lower than 7.4, only ACP precipitation does not represent the experimental points, so the co-precipitation with DCPD and ACP is proposed.

Only the final stage of the calcium phosphate precipitation is considered. Note also that solid–solid transformations are not taken into account. The situations assumed here are based on non-dissolution of the less stable phase.

The precipitation of ACP can be written as follows:

$$3Ca^{2+} + 2PO_4^{3-} \longrightarrow Ca_3(PO_4)_2 \qquad (4)$$

Table 3. Required time for total transformation of calcium phosphate in HAP as function of pH (Boskey and Posner, 1973).

pH	Time (min)
6.8	60
7.0	130
7.5	255
8.0	400
9.0	410
10.0	700

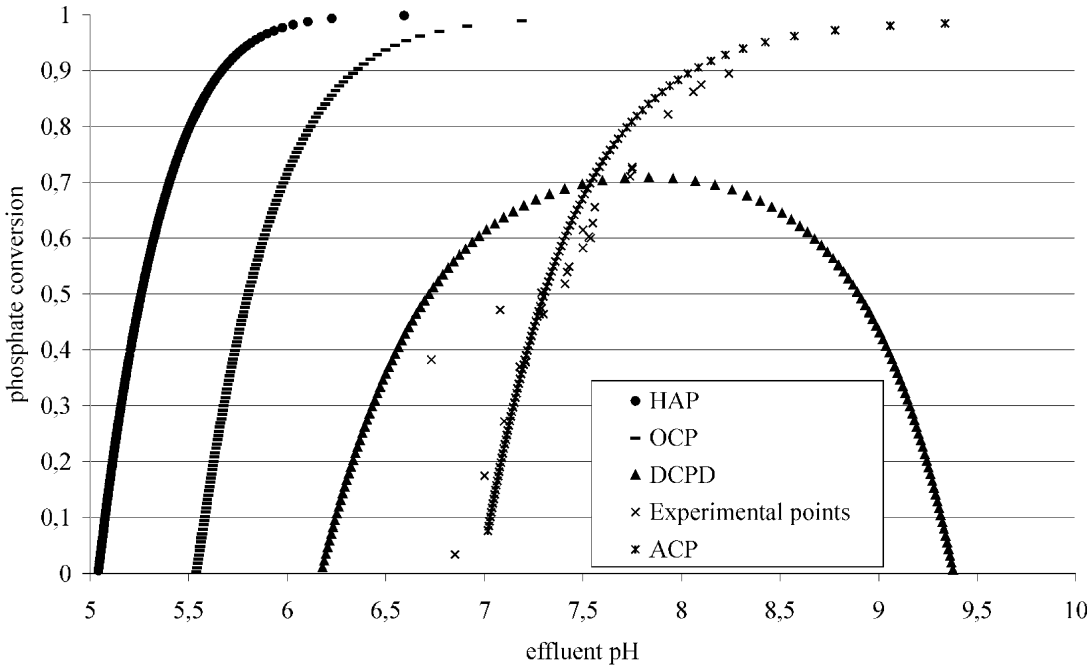

Figure 3. Identification of the species for calcium phosphate precipitation.

The ACP supersaturation is defined by the β parameter, set at equilibrium (i.e. taken equal to zero) which is:

$$\beta_{ACP} = \frac{1}{5}\ln\left(\frac{([Ca^{2+}]\lambda_{Ca^{2+}})^3([PO_4^{3-}]\lambda_{PO_4^{3-}})^2}{Ks_{ACP}}\right) \quad (5)$$

The model inputs are the concentrations of calcium, phosphate and KOH.

The model is then used to determine if precipitation of DCPD is possible in these new conditions according to the following reaction:

$$Ca^{2+} + HPO_4^{2-} \longrightarrow CaHPO_4 \quad (6)$$

For this purpose, the phosphate mass balances and the electroneutrality equation for DCPD precipitation are solved and the DCPD supersaturation is computed according to Equation (7):

$$\beta_{DCPD} = \frac{1}{2}\ln\left(\frac{([Ca^{2+}]\lambda_{Ca^{2+}})([HPO_4^{2-}]\lambda_{HPO_4^{2-}})}{Ks_{DCPD}}\right) \quad (7)$$

It means that if DCPD supersaturation is greater than zero, precipitation of DCPD is likely to occur. The model outputs are the conversions of both ACP and DCPD, the concentrations of the different ions and pH. A flowchart (Figure 4) illustrates the principle of the proposed method for calcium phosphate precipitation.

The concentrations of ions and complexes are determined from chemical equilibrium relations (see Table 4; Montastruc *et al.*, 2002b). A sensitivity analysis has further shown that the complexes involving potassium and chloride ions do not affect substantially the chemical equilibrium and are thus neglected.

Consequently, the system to be solved for ACP precipitation contains 12 non-linear equations with 12 variables, i.e. concentrations of the aqueous species (11) and conversion. This set of equations was solved by a Newton–Raphson method. Since a difficult initialization phase is involved in the numerical resolution of the above-mentioned set of equations, the number of equations was reduced to the four balance equations. The final unknowns of the system were thus only the concentrations $[Ca^{2+}]$, $[PO_4^{3-}]$, $[H^+]$ and the phosphate conversion. The system of equations was solved for various initial KOH concentrations in order to analyse the influence of pH on conversion. Since calcium is fed in the form of calcium chloride, the chloride concentration was taken as equal to 2 $[Ca^{2+}]$.

The Debye–Huckel model giving the activity coefficient of each species was used in this study:

$$\log_{10}\lambda = -A_{DH}z_i^2\frac{\sqrt{\mu}}{1 + B_{DH}\alpha\sqrt{\mu}} + C_{DH}\mu \quad (8)$$

where

$$B_{DH} = \sqrt{\frac{2e^2N_A\rho_o}{\varepsilon k_B T}}$$

and C_{DH} is a constant equal to $0.055\,mol\,l^{-1}$.

A preliminary study was performed to determine the influence of equilibrium constants and activity model on equilibrium (Montastruc *et al.*, 2002b). The main result was that the activity model had no influence but the sensitivity of the equilibrium constant was very important.

Reactor Network Model

The second step of the proposed methodology involves the computation of the pellet reactor efficiency. This phase has been achieved by the identification of the pellet reactor as a reactor network involving a combination of elementary systems representing basic ideal flow patterns (perfect mixed flows, plug flows, etc.; see Figure 5).

The combination of elementary systems representing basic ideal flow patterns is described by a superstructure (Floquet *et al.*, 1989). It contains four perfect mixed flows arranged in series, two plug flows, one by-pass, two dead

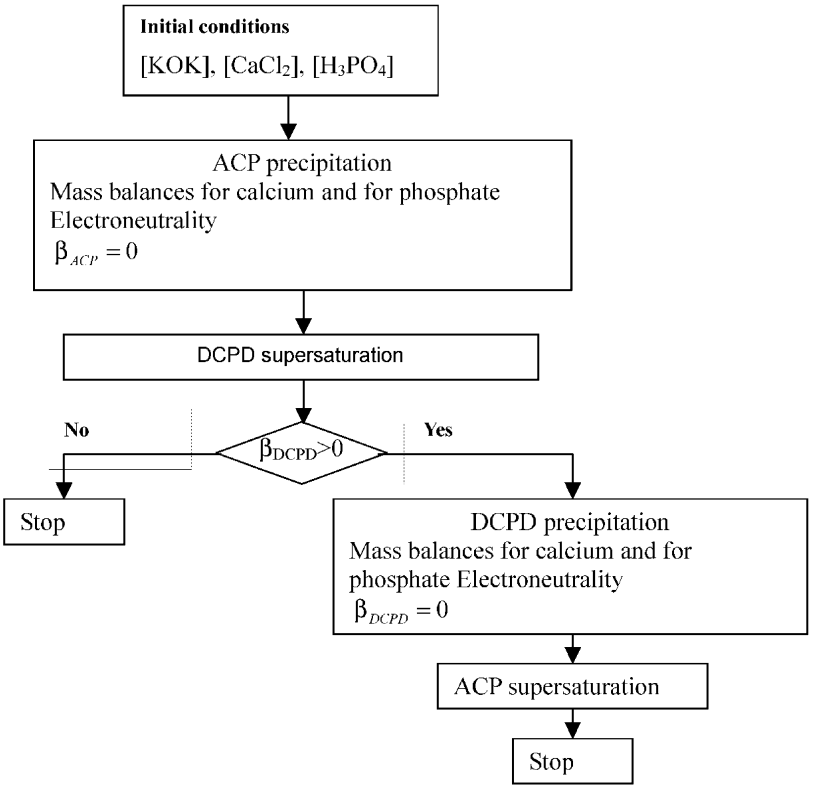

Figure 4. Principle of the method proposed for modeling calcium phosphate precipitation.

volumes (i.e. without reaction) and one recycling flow and represents the different flow arrangement (integer variables) that is likely to take place in the fluidized bed. Let us recall that more than four series of perfect mixed flows produce the same effect as a plug flow.

The precipitation phenomenon is described as an agglomeration of fines particles on large grains, which is represented by Smoluchowski's equation (Mullin, 2001).

$$\frac{dN_i}{dt} = -kN_iN_j \; (i = \text{fines}, j = \text{grains}) \tag{9}$$

which can easily be written in an equivalent form as follows:

$$\frac{dC_i}{dt} = -KC_iN_j \tag{10}$$

where N is the particle concentration (m^{-3}) and C is the concentration (mg m^{-3}). K and k represent kinetic constants ($m^{-3}\,s^{-1}$).

$$N_j = \frac{1-\varepsilon}{(4/3)\pi r_j^3} \tag{11}$$

Table 4. Equilibrium constants for the system Ca–PO_4–H_2O, $K_i = [(A_i)(B_i)]/(AB_i)$.

K_i	A_i	B_i	AB_i	K_i value
K_1	H^+	$H_2PO_4^-$	H_3PO_4	7.1285×10^{-3}
K_2	H^+	HPO_4^-	$H_2PO_4^-$	6.2373×10^{-8}
K_3	H^+	PO_4^-	HPO_4^-	453.942×10^{-15}
K_4	Ca^{2+}	$H_2PO_4^-$	$CaH_2PO_4^+$	3.908×10^{-2}
K_5	Ca^{2+}	HPO_4^-	$CaHPO_4$	1.8239×10^{-3}
K_6	Ca^{2+}	PO_4^-	$CaPO_4^-$	347.536×10^{-9}
K_7	Ca^{2+}	OH^-	$CaOH^+$	5.8884×10^{-2}
K_w	H^+	OH^-	H_2O	1.004×10^{-14}

The bed porosity ε is calculated using a modified Kozeny–Carman equation (van Dijk and Wilms, 1991):

$$\frac{\varepsilon^3}{1-\varepsilon} = 130\left(\frac{v_{sup}^{1.2}\upsilon^{0.8}}{g(2r_j)^{1.8}}\right)\left(\frac{\rho_l}{\rho_S - \rho_l}\right) \tag{12}$$

where r_j is the grain radius, v_{sup} the superficial velocity (m s^{-1}), υ the kinematic viscosity ($m^2\,s^{-1}$) and ρ the density (kg m^{-3}).

The continuous variables are the 'kinetic' constant (K), the flowrate, equation (5), and the reactor volumes, equation (8). In fact, the superstructure represents the hydrodynamical conditions in the fluidized bed. The kinetic constant is obtained for each combination generated by the simulated annealing algorithm. This kinetic constants depends only on the precipitation temperature and not on flowrate and sand amount. A summary of the global methodology for computating the efficiency is presented in Figure 2.

At the upper level of the procedure, the scheduling of the basic structures is first optimized by a simulated anneal (SA). The simulated annealing procedure mimics the physical annealing of solids, that is, the slow cooling of a molten substance, that redistributes the arrangement of the crystals (Kirkpatrick *et al.*, 1983). The SA algorithm implemented in this study involves these classical procedures. The dynamic management of the different constraints generated by the structures induced by the stochastic simulated annealing algorithm is then solved by a quadratic programming algorithm (QP) (QP package from the IMSL library). At the lower level, the set of parameters is identified for a given structure by QP. The J objective function for QP is to

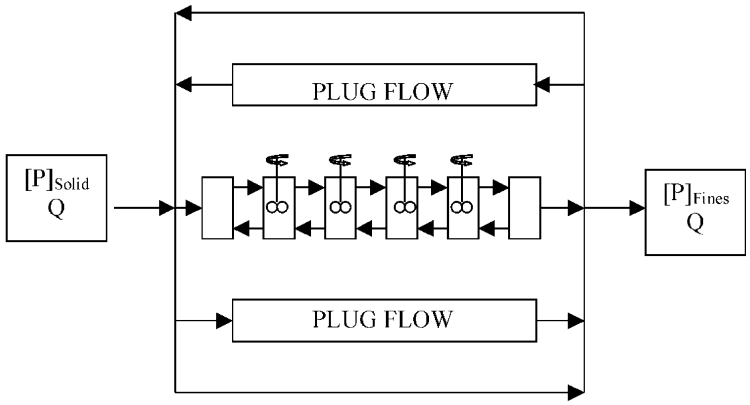

Figure 5. Superstructure detail.

minimize the square distance between the experimental and the computed points.

$$J = \min[(\eta_{\mathrm{agg}_{\mathrm{exp}}} - \eta_{\mathrm{agg}_{\mathrm{mod}}})^2] \tag{13}$$

For SA, the criterion S is based on minimization of the QP function with a penalty term proportional to the complexity of the tested structure. The SA parameters are the length of the cooling stage (*Nsa*), the initial structure and the reducing temperature factor (α). The usual values for *Nsa* are between eight and two times the chromosome length whereas the values for α are between 0.7 and 95. The *Nsa* and α values used in this study are, respectively, 6 and 0.7.

$$S = \min\left[(\eta_{\mathrm{agg}_{\mathrm{exp}}} - \eta_{\mathrm{agg}_{\mathrm{mod}}})^2 + \rho \sum_j y^2\right] \tag{14}$$

EXPERIMENTAL POINTS AND VALIDATION

Phosphate Conversion

Experimental points have been used to validate the approach (Figure 6). They correspond to an initial phosphorus concentration of 50 mg l^{-1}, a Ca/P molar ratio equal to 3 and a temperature equal to 20°C. The simulation fitting was carried out by adjusting the solubility constant values of both mineral species (ACP and DCPD).

The pK value for ACP which corresponds to the best fitting of the experimental results is equal to 25.297 for pH values higher than 7.4. This pK value has the same order of magnitude than the average one reported in the literature (see Table 1; Montastruc *et al.*, 2002). The pK value for DCPD is fixed to 6.346 when considering the zone for pH lower than 7.4, thus implying precipitation of ACP and also DCPD, in order to adjust the model with the experimental points (Figure 6). For pH values lower than 7.4, only ACP is assumed to precipitate. This case is probably due to the fact that the CaP particles were not agglomerated

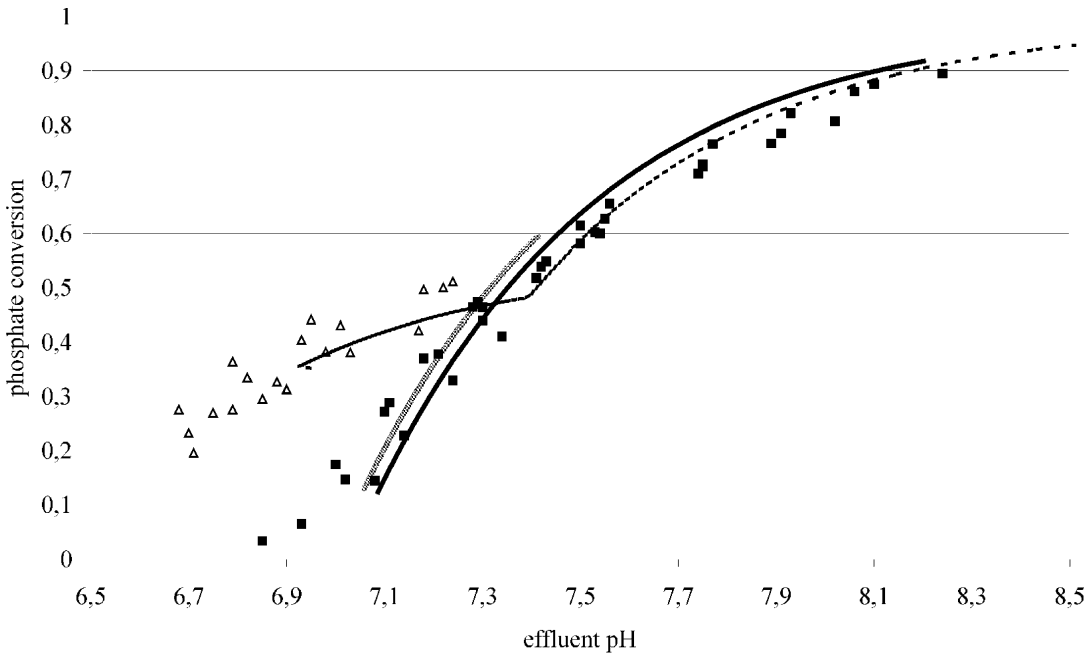

Figure 6. Phosphate conversion vs. effluent pH.

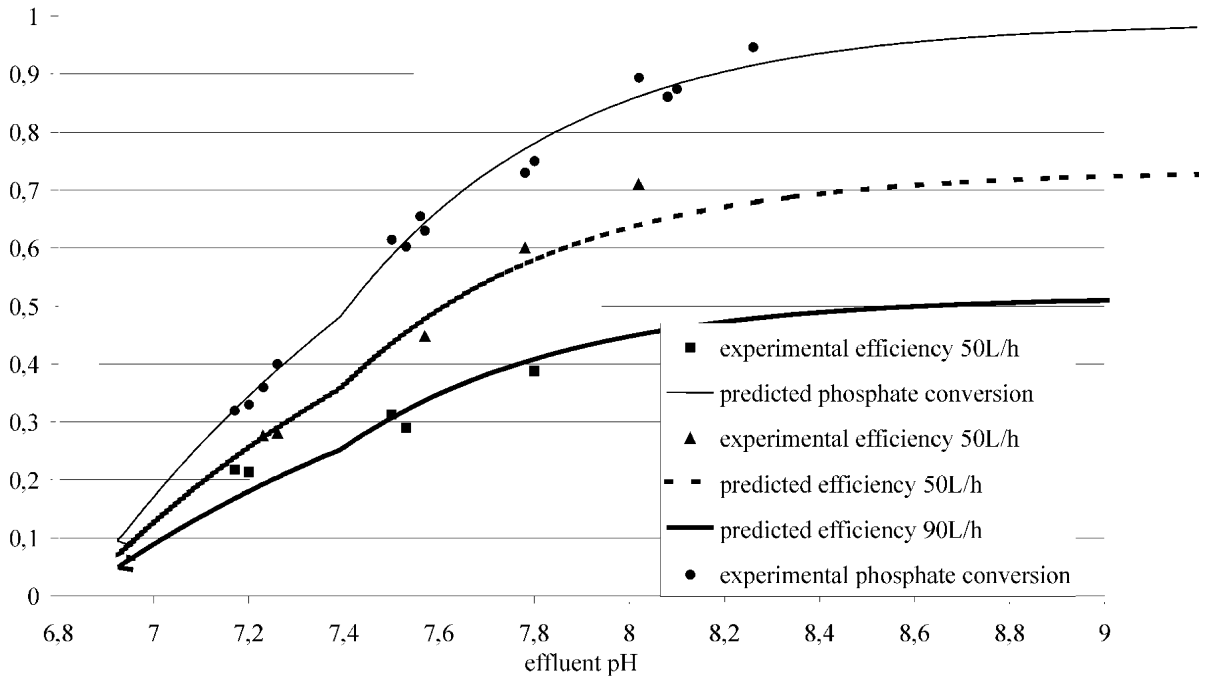

Figure 7. Phosphate efficiency vs. effluent pH.

Table 5. Comparison between experimental and modeling results.

	Case 1	Case 2
Penalty term	10^{-6}	0
Experimental η_{agg}		
for 50 l h^{-1}	0.742	0.742
90 l h^{-1}	0.523	0.523
Total Reactor volume		
for 50 l h^{-1}	1.91	1.91
90 l h^{-1}	1.31	1.31
Modeling η_{agg}		
for 50 l h^{-1}	0.7396	0.7423
90 l h^{-1}	0.5242	0.5231
Error	0.2%	0.01%
Kinetic constant	4.830	4.451

around the sand grains (clean sand) and no DCPD precipitation was observed. In this case, the pK was taken equal to 25.476.

Phosphate Efficiency

The agglomeration rate represented by a first order equation has also been identified with experimental runs (see Figure 7). The experimental rate has been determined for each flow rate by minimization of the square distance for each point between the experimental efficiency and the computed efficiency [see relation (3)].

In this study, two cases have been studied to show the influence of different penalty terms for two values of total flowrate of the solution to be treated (50 and 90 l h^{-1}).

The results obtained show that the resulting combination depends strongly on the penalty term. On the one hand, it is interesting to notice that if the penalty term is very low or equal to zero, the resulting error is also low but the combination is more complicated than the one obtained with a higher penalty term (Table 5; see Figure 8). On the other hand, this combination induced a more important error between the computed and experimental results, thus suggesting that the method is sensitive to the required precision. For 100 runs of SA, the CPU time is the same for the two cases, that is 7 min (4.2 s for each SA) on a PC architecture.

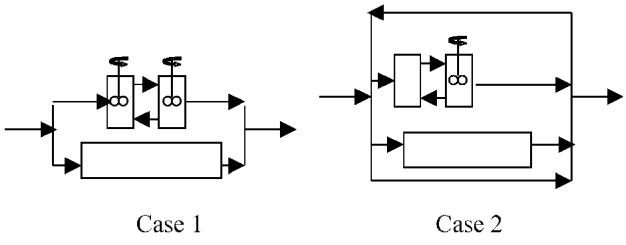

Figure 8. Best combination obtained for two values of the penalty term.

DISCUSSION AND CONCLUSIONS

A two-stage methodology was proposed in this paper pellet reactor modeling used for P recovery by calcium phosphate precipitation. The first model is a thermodynamical one while the second represents the hydrodynamic case in the fluidized bed. Note that the initial parameters of second model are the outlet values of the thermochemical one.

This study improves the understanding of the precipitation of two calcium phosphates in either neutral or basic environment from a thermodynamical viewpoint. It gives for high pH values a domain in which only ACP precipitation is likely to occur and for neutral pH values a zone in which conditions of precipitation of ACP and DCPD are likely to take place. The model only takes into account thermodynamic concepts. The model developed in this study is now used for validation and determination of process operating conditions for phosphate precipitation in a fluidized-bed reactor. The major interest of this model is to evaluate both quantitatively and qualitatively the precipitated calcium phosphates.

Moreover, a hybrid optimization technique combining an SA and a QP method has been developed for identification of a reactor network which represents the pellet reactor for P recovery, viewed as a mixed integer programming problem. Two levels are involved: at the upper level, the SA generates different combinations and at the lower level, the set of parameters is identified by a QP method. The results show that, for the two values of the total flowrate of the solution to be treated, a simple combination of ideal flow patterns is found, which is interesting for the future control of the process.

NOMENCLATURE

e	electronic charge ($=1.602177\times10^{-19}$ C)
k_B	Boltzmann constant ($=1.380658\times10^{-23}$ J K^{-1})
N_A	Avogrado number ($=6.022136\times10^{23}$ mol^{-1})
T	temperature, K
z_i	charge number of ion

Greek symbols

ε	solvent dielectric constant ($\varepsilon=\varepsilon_r*\varepsilon_o$)
ε_o	vacuum permitivity ($=8.854187\times10^{-12}$ F m^{-1})
ε_r	relative solvent dielectric constant
λ	ion activity coefficient
ρ_o	solvent density, kg m^{-3}
μ	solution ionic strength, mol l^{-1}

REFERENCES

Baronne, J.P. and Nancollas, G.H., 1977, The seeded growth of calcium phosphates: the effect of solid/solution ratio in controlling the nature of growth phase, *J Colloid Interface Sci*, 62(3): 421–431.

Boskey, A.L. and Posner, A.S., 1973, Conversion of amorphous calcium phosphate to microcrystalline hydroxyapatite. A pH-dependent, solution-mediated, solid–solid conversion, *J Phys Chem*, 77(7): 2313–2317.

Floquet, P., Pibouleau, L. and Domenech, S., 1989, Identification de modèles par une méthode d'optimisation en variables mixtes, *Entropie*, 151: 28–36.

Freche, M., 1989, Contribution à l'étude des phosphates de calcium: croissance sur le phosphate dicalcique anhydre: croissance de dépôts élaborés par pulvérisation chimique. Thèse INPT.

Hirasawa, I. and Toya, Y. 1990, Fluidized-bed process for phosphate removal by calcium phosphate crystallization, *ACS Symp Ser*, 438: 355–363.

Kirkpatrick, S., Gellat, C.D. and Vecci, M.P., 1983, Optimization by simulated annealing, *Science*, 220: 671–680.

Meyer, J.L. and Eanes, E.D., 1978, A thermodynamic analysis of the amorphous to crystalline calcium phosphate transformation, *Calc Tiss Res*, 25: 59–68.

Montastruc, L., Azzaro-Pantel, C., Cabassud, M. and Biscans, B., 2002a, Calcium phosphate precipitation in a pellet reactor, in *15th International Symposium on Industrial Crystallization*, Sorrento, 15–18 September.

Montastruc, L., Azzaro-Pantel, C., Biscans, B., Cabassud, M. and Domenech, S., 2002b, A thermochemical approach for calcium phosphate precipitation modeling in a pellet reactor, *Chem Eng J* (in press).

Morse, G.K., Brett, S.W., Guy, J.A. and Lester J.N., 1998, Phosphorus removal and recovery technologies, *Sci Total Environ*, 212(1): 69–81.

Mullin, J.W., 2001, *Crystallization*, 4th edn (Butterworth-Heineman, Oxford, UK).

Ringbom, A., 1967, *Les Complexes en Chimie Analytique* (Dunod, Paris).

Seckler, M.M., Bruisma, O.S.L. and van Rosmalen, G.M., 1996a, Calcium phosphate precipitation in a fluidized bed in relation to process conditions: a black box approach, *Water Resources*, 30(7): 1677–1685.

Stumm, W. and Morgan, J.J., 1981, *Aquatic Chemistry, an Introduction Emphasizing Chemical Equilibria in Natural Waters*, 2nd edn (Wiley, New York, USA).

van Dijk, J.C. and Wilms, D.A., 1991, Water treatment without waste material. Fundamental and state of the art of pellet softening, *J Water SRT Aqua*, 49: 263–280.

Van Kemenade, M.J.J.M. and de Bruyn, P.L., 1987, A kinetic study of precipitation from supersatured calcium phosphate solutions, *J Colloid Interface Sci*, 118(2): 564–585.

ACKNOWLEDGEMENTS

The authors are grateful to 'the Direction Régionale de la Recherche et de la Technologie' of Midi-Pyrénées for its financial support to this study.

ADDRESS

Correspondence concerning this paper should be addressed to Dr L. Montastruc, Laboratoire de Génie Chimique-UMR 5503 CNRS/INP/UPSENSIACET, 118 Route de Narbonne 31 Toulouse cedex 4, France. E-mail: ludovic.montastruc@ensiacet.fr

The paper was presented at the 9th Congress of the French Society of Chemical Engineering held in Saint-Nazaire, France, 9–11 September 2003. The manuscript was received 20 February 2003 and accepted for publication after revision 8 September 2003.